GEOPHYSICAL RESEARCH LETTERS, VOL 22, NO. 13, PAGES 1741-1744, JULY 1, 1995

Ponderomotive saturation of magnetospheric field line resonances

R. Rankin, P. Frycz, V. T. Tikhonchuk[1], and J. C. Samson

Department of Physics, University of Alberta, Edmonton, Canada

Abstract. Compressional Alfvén waves in the terrestrial magnetospheric cavity constitute a discrete spectrum of global modes which can resonate with specific components of the continuum spectrum of shear Alfvén wave (SAW) field line resonant frequencies. We investigate the effect of the ponderomotive force (PF) of excited standing SAWs on the nonlinear saturation of field line resonances (FLRs). In low β plasmas FLR saturation occurs due to a nonlinear phase slip between the fast mode driver and SAW field. Ponderomotive forces also lead to density depletions at the ionospheres, nonlinear narrowing of the FLR and meridional scales comparable to those embedded within temporally modulated discrete auroral arcs. Observational features relating to these effects are discussed.

Introduction

Field line resonances are standing shear Alfvén waves in the Earth's magnetosphere, and can be formed through resonance absorption of global mode compressional or impulsively driven Alfvén waves in the magnetospheric cavity. Near the ionosphere, FLRs often have latitudinal scale sizes comparable to the scale size of discrete arcs, 50km or less, and experimental evidence suggests that optical emissions from auroral arc structures can be modulated by MHD waves propagating along the Earth's magnetic field lines [Xu, Samson and Liu 1993]. With electron inertia and parallel electric fields, MHD FLRs can perhaps explain observations of accelerated electrons and discrete forms (5km scales or less) embedded within auroral arcs [Mozer 1981, Goertz 1984]. FLRs are often associated with intensifications of arcs and observations suggest that large amplitude FLRs are susceptible to nonlinear Kelvin Helmholtz instabilities [Samson and Rankin 1994]. In the solar chromosphere, resonance absorption of SAWs has been presented as a viable mechanism for heating of the solar corona [Ionson 1978, Ofman, Davila and Steinolfson 1994].

In this paper we present a new nonlinear mechanism of saturation of standing wave FLRs, and describe a process which can lead to perpendicular scales in FLRs comparable to the discrete forms observed within certain auroral arc structures. We show that the expected scales from our model should be comparable to the electron inertia length. The nonlinear mechanism that we consider is related to the PF of SAWs. The PF is especially important for standing SAWs, and can perhaps explain the origins of atomic Oxygen at high altitudes [Li and Temerin 1993]. During resonance absorption, the PF of the excited SAW changes the local plasma density, which evolves as a slow magnetosonic wave (SMW), and causes a temporal change in the eigenfreqency of the SAW. A frequency mismatch with the compressional driver develops and leads to saturation of the excited SAW. The change in the plasma density also leads to a spatial shift of the resonance layer and results in strong nonlinear narrowing of the FLR. Temporal dephasing on adjacent magnetic field lines leads to very short perpendicular scales across the FLR.

In Rankin et al. [1994], and Tikhonchuk et al. [1995] we presented a theoretical framework for describing nonlinear PF effects in simple plane SAWs excited by a constant amplitude driver in a homogeneous plasma. In the present article, we extend our models to 3-D inhomogeneous plasmas, and verify them using numerical solutions to the resistive MHD equations. We derive analytical expressions for the amplitude and time of ponderomotive saturation of FLRs, compare them with the simulations, and discuss observational consequences of our model. Our findings agree with rocket observations of large density depletions associated with SAWs [Boehm et al. 1990], and with recent numerical simulations [Ofman, Davila, and Steinolfson, 1994].

Nonlinear Model of Standing SAWs

Our starting point is the standard system of resistive MHD equations, where the density, ρ_0, is inhomogeneous in the x-direction and the external magnetic field $\mathbf{B}_0(x)$ is directed along the z-axis:

$$\rho\left(\frac{\partial}{\partial t}+\mathbf{V}\cdot\nabla\right)\mathbf{V}=-\nabla P+\mathbf{J}\times\mathbf{B}+\nu\nabla^2\mathbf{V},$$

$$\nabla\times\mathbf{E}=-\frac{\partial\mathbf{B}}{\partial t},\qquad \nabla\times\mathbf{B}=\mu_0\mathbf{J}, \tag{1}$$

$$\mathbf{E}+\mathbf{V}\times\mathbf{B}=\eta\mathbf{J},\qquad \frac{\partial\rho}{\partial t}+\nabla\cdot(\rho\mathbf{V})=0.$$

Here, ν and η are the viscosity and resistivity, respectively, and all other symbols have their usual meanings. We address here ULF waves and ignore the Hall and

[1]On leave from the P. N. Lebedev Physics Institute, Russian Academy of Sciences, Moscow.

Paper number 95GL01311
0094-8534/95/95GL-01311$03.00

electron inertia terms in Ohm's law. Considering for the moment the linear approximation to Eqs. (1), we assume that $\beta \equiv 2\mu_0 P_0/B_0^2 \ll 1$ and that dissipation effects are small. A straightforward calculation leads to equations for the wave magnetic field $\mathbf{b} = \mathbf{B} - \mathbf{B_0}$ and plasma displacement, $\boldsymbol{\xi}$,

$$\left(\frac{1}{V_A^2}\frac{\partial^2}{\partial t^2} + \frac{\Gamma_A}{V_A^2}\frac{\partial}{\partial t} - \frac{\partial^2}{\partial z^2}\right)\xi_x = -\frac{1}{B_0}\frac{\partial b_z}{\partial x}, \quad (2)$$

$$\left(\frac{1}{V_A^2}\frac{\partial^2}{\partial t^2} + \frac{\Gamma_A}{V_A^2}\frac{\partial}{\partial t} - \nabla^2\right)b_z = B_0\frac{\partial^2\xi_x}{\partial t^2}\frac{d}{dx}\frac{1}{V_A^2}, \quad (3)$$

where $V_A(x) = \sqrt{B_0^2/\mu_0\rho_0}$, $\Gamma_A = -\frac{1}{2}(\eta/\mu_0 + \nu/\rho_0)\nabla^2$ and $\boldsymbol{\xi}$ is defined through $\mathbf{V} = \partial\boldsymbol{\xi}/\partial t$.

In an inhomogeneous plasma, an external source of frequency ω and field-aligned wave number k_z excites SAWs at the critical layer $x = x_c$ where the resonance condition $V_A^2(x_c) = \omega^2/k_z^2$ is satisfied. For low azimuthal wave numbers the largest enhancement is experienced by the shear components b_y and ξ_y. From Eq. (1), ξ_y can be expressed in terms of b_z according to:

$$\left(\frac{1}{V_A^2}\frac{\partial^2}{\partial t^2} + \frac{\Gamma_A}{V_A^2}\frac{\partial}{\partial t} - \frac{\partial^2}{\partial z^2}\right)\xi_y = -\frac{1}{B_0}\frac{\partial b_z}{\partial y}. \quad (4)$$

Eqs. (2-4) can be solved if we assume standing waves along z, Fourier transform in y, and envelope the equations over the frequency ω. The z-component of $\mathbf{b}$ and the x- and y-components of $\boldsymbol{\xi}$ are then represented as $A(x,y,z,t) = \mathrm{Re}[A(x,t)\exp(i\omega t - ik_y y)]\sin(k_z z)$, where $A(x,t)$ changes slowly in time with respect to the driver period. The x- and y- components of $\mathbf{b}$ have a cosine dependence on z along $\mathbf{B_0}$.

To proceed further we must incorporate nonlinear effects. Since coupling between compressional and SAWs is strongest near to the resonance point, x_c, we may approximate $V_A^2(x)$ there by a linear function,

$$\frac{1}{V_A^2} \approx \frac{k_z^2}{\omega^2}\left(1 - \frac{x - x_c}{L} + \frac{\delta\rho}{\rho_0}\right), \quad (5)$$

where L is the scale length of V_A around x_c and $\delta\rho(\mathbf{r},t)$ is the PF density perturbation. By virtue of the envelope approximation, the PF drives second spatial harmonic, $(k_y = 0, 2k_z)$, density perturbations of the form, $\delta\rho/\rho_0 = n\cos(2k_z z)$. The amplitude $n(x,t)$ satisfies the driven SMW equation [Tikhonchuk et al. 1995]

$$\left(\frac{\partial^2}{\partial t^2} + 2\Gamma_S\frac{\partial}{\partial t} + 4k_z^2 C_S^2\right)n = -\frac{\omega^2}{2B_0^2}b_y^2. \quad (6)$$

Here, $C_S = \sqrt{\delta P/\delta\rho}$ is the sound speed and $\Gamma_S = -(\nu/2\rho_0)\nabla^2$ describes damping of the SMW. In the resonance region, only the dominant term b_y is kept on the right hand side. Using Eq. (5), the envelope approximation, and the relationships $b_{x,y} = k_z B_0 \xi_{x,y}$, nonlinear equations describing the wave amplitudes in Eqs. (2-4) can be derived. The main nonlinear effects appear in b_y, which is described according to,

$$\left(\frac{2i}{\omega}\frac{\partial}{\partial t} + \frac{2i}{\omega}\Gamma_A + \frac{x - x_c}{L} + \frac{1}{2}n\right)b_y = i\frac{k_y}{k_z}b_z. \quad (7)$$

According to Eq. (6) the PF produces density depletions in the anti-nodes of b_y. From Eq. (7) this leads to an Earthward shift of the resonant layer, $x_{res} \to x_c - Ln/2$. This nonlinear effect is a result of frequency detuning and leads to saturation of the SAW.

Near to the critical layer $x = x_c$, b_z can be shown to be approximately constant, $b_z(x) \approx b_c[1 + (q/2)\zeta^2\ln\zeta]$, where $q = (k_z L)^{2/3}k_y^2/k_z^2$ and $\zeta = (x - x_c)k_z^{2/3}/L^{1/3}$. The right hand side of Eq. (7) can then be treated as a constant source $ib_c k_y/k_z$ which drives b_y. This equation for b_y, together with Eq. (6), reduces to the system of equations for nonlinear driven SAWs studied in Tikhonchuk et al. [1995] (cf. Eq. (18) of that paper):

$$\dot{b} + \Gamma_A b = i\left(\Delta\omega - \frac{1}{4}\omega n\right)b + \frac{1}{2}R\omega,$$
$$\ddot{n} + 2\Gamma_S\dot{n} + \Omega^2 n = -\frac{1}{2}\omega^2|b|^2, \quad (8)$$

where $b(t) = b_y/B_0$. Here, the dimensionless driver strength is $R = k_y b_c/k_z B_0$ and $\Delta\omega(x) = \omega(x_c - x)/2L$ is a spatial linear frequency detuning parameter. Eq. (8) describes coupling between a SAW and a SMW. The SAW experiences a nonlinear frequency shift, $\omega n/4$, proportional to the amplitude of the SMW, and the SMW is driven by a PF that is proportional to the intensity of the SAW. As explained in Tikhonchuk et al. [1995], the system (8) has two characteristic times: one timescale is related to the period of the driven SMW, $\pi/k_z C_s$, and the other is associated with the characteristic timescale for nonlinear effects.

Analysis and Full MHD Solutions

We review the linear predictions of our model by ignoring the density perturbation in Eqs. (8). Then, the dissipative saturation time, t_{ds}, and the saturated magnetic field amplitude are easily found to be:

$$t_{ds} \approx 4\pi\left(\frac{L}{\omega}\right)^{\frac{2}{3}}\left(\frac{\eta}{\mu_0} + \frac{\nu}{\rho_0}\right)^{-\frac{1}{3}}, \quad b_{y,ds} \approx \tfrac{1}{2}B_0 R\omega t_{ds}. \quad (9)$$

If FLR dissipation is small, the linear saturation level, Eq. (9), may be quite large and nonlinear effects will become important. We can then apply the results of Tikhonchuk et al. [1995] to the FLR case and summarize our model in the following way. Linear saturation of FLRs will occur for $R < 8(\beta\gamma)^{1/2}(\Gamma_A/\omega)^{3/2}$, where γ is the adiabatic index. Otherwise, ponderomotive saturation of the SAW magnetic field $b_{y,max}$, velocity $v_{y,max}$, and density perturbation, n_{max}, will occur in a time t_{sat} determined by:

$$b_{y,max} = 2B_0 R^{3/5}, \quad n_{max} = 2R^{6/5}/\beta\gamma,$$
$$v_{y,max} = 2V_A R^{3/5}, \quad t_{sat} = 6\omega^{-1}R^{-2/5}. \quad (10)$$

After the saturation time (10), nonlinear temporal de-

phasing on adjacent field lines across the FLR will lead to radial structuring of the resonance layer. This will continue until dissipative or non-ideal MHD effects become important.

Now we compare our results with solutions to the full set of 3-D MHD equations defined by Eq. (1). We use a Cartesian model of the dipole magnetosphere, which accounts for the dominant effects of resonant wave conversion and plasma parallel motion due to the PF. Numerical techniques used to solve the MHD equations are detailed in Rankin, Samson and Frycz [1993]. We apply periodicity conditions in y- and z, and in the x-direction an incident fast mode is applied at $x = 0$. The gradient in $V_A(x)$ is due to a spatially varying density profile. We take $k_y \approx k_z$ and a density profile, $\rho_0(x)$, with a scale length corresponding to maximum absorption.

Taking $\gamma\beta = 0.011$, and an incident wave flux at $x = 0$ corresponding to $R \approx 0.01$, the saturation timescale, according to Eq. (10), is approximately 6 SAW periods, and the saturated amplitude of the magnetic field, b, is approximately $0.13B_0$. We again note that saturation occurs due to the nonlinear frequency shift $\omega n/4$ in the system (8). When the nonlinear phase shift reaches $\pi/2$, the SAW amplitude will saturate.

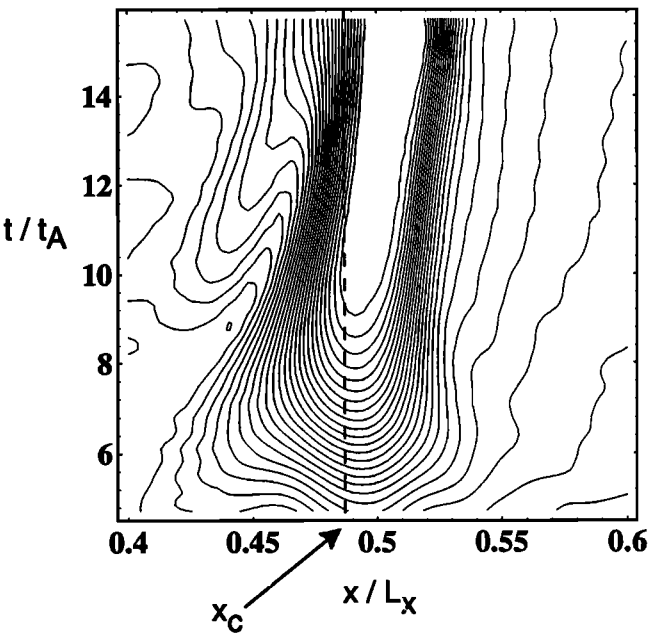

Figure 2. Contours of Fourier amplitude of $b = b_y/B_0$. The horizontal axis is normalized to the length of the system, $L_x = 8L$, in the simulations.

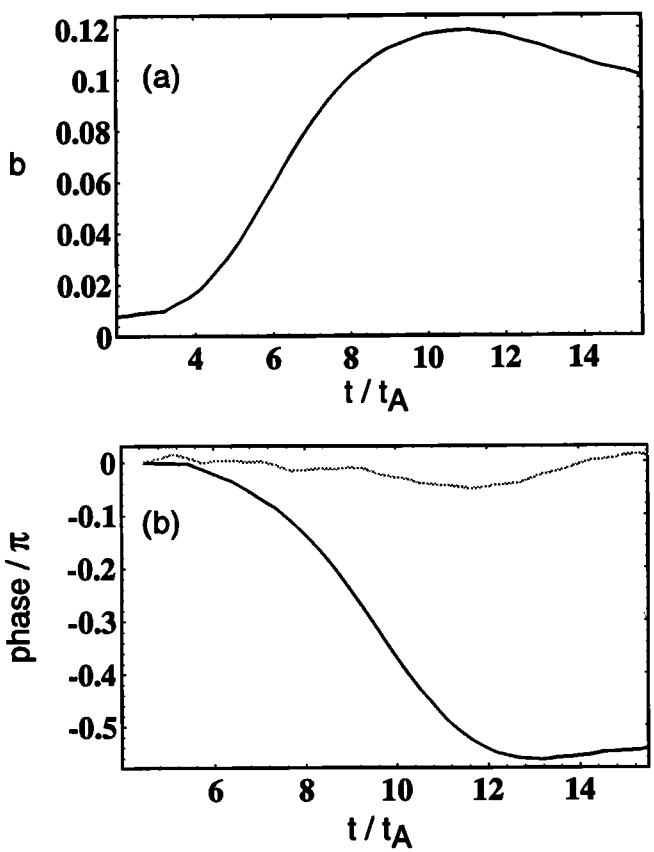

Figure 1. Numerical solution to Eqs. (1) with $\gamma\beta = 0.011$ and $R = 0.01$. (a) Fourier amplitude of $b = b_y/B_0$, (b) phase shift between driver and SAW at the linear resonance position (dark line), and at a point outside of the resonance (faint line). The time axis is normalized to the period t_A of the SAW and starts at $t > 0$ after the phase becomes well defined.

This occurs in Fig. 1(a), which shows the Fourier amplitude of b_y at the linear resonance position as a function of time. The incident wave field has been ramped up linearly from small amplitude to $b_y = 0.01$ over 4.5 Alfvén periods, so that with respect to this time, saturation occurs in approximately 6 periods. Fig. 1(b) shows the nonlinear phase shift at the linear resonance position, and at a point outside of the resonance. The saturated amplitude and phase shift agree with the theory.

Our nonlinear model predicts strong nonlinear temporal dephasing between the excited SAW and driver. This is a consequence of a spatial shift of the resonance due to PF density perturbations. Fig. 2 shows contours of the amplitude of $b_y(x,t)$ in $x - t$ space. The position of the FLR predicted by linear theory is at $x/L_x = 0.486$ in these units, and it can be seen that the resonance nonlinearly shifts to $x/L_x = 0.51$ over the time simulated. Since the FLR has a tendency to narrow as it shifts position, the maximum shift is on the order of the width of the resonance predicted by the theory, $\delta x \sim L\sqrt{\beta\gamma} \sim 0.1L$. In Fig. 2, for $t > t_{sat}$ the maximum amplitude of b_y is constant at $0.12B_0$.

Now we consider the behavior of the system according to the simplified set of equations (8). In the absence of damping the full x-dependence of the FLR can be constructed by solving the model equations, Eq. (8), for each position x, with $V_A(x)$ used to specify the detuning parameter $\Delta\omega(x) = \omega(x_c - x)/2L$. This is illustrated in Fig. 3, which shows b_y (with no separation of amplitude and phase) as a function of position x. The faint line indicates the wave field near the time of nonlinear saturation, Eq. (10), and the darker line corresponds to a situation approximately two nonlinear saturation times later. Following the initial time of saturation, the devel-

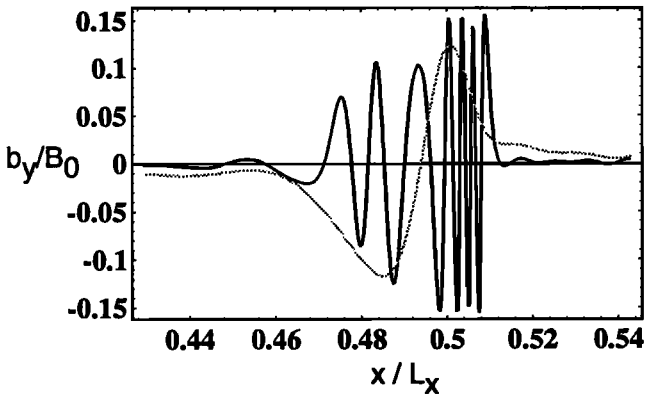

Figure 3. b_y as a function of x/L_x ($L_x = 8L$) from the model equations with $\gamma\beta = 0.0025$. The faint line shows the FLR near the time of nonlinear saturation. The solid line corresponds to $t = 3t_{sat}$.

opment of the phase slip between the driver and SAW (at each x-position) leads to very short scales in the perpendicular direction. To resolve these short scales one must go outside of ideal MHD and include perhaps finite electron inertia effects. This is not addressed here.

The absence of significant radial structuring of the amplitude in the numerical solutions to Eq. (1) can be explained by noting that a small amount of damping is necessary in the computational algorithm in order to stabilize the code. The effect of this damping is to remove the time history of the phase of the SAW (on a particular field line) after a time comparable to the timescale for resistive diffusion. In the 3-D simulations, the dissipation times and corresponding length scales are sufficient for nonlinear saturation to occur, but cannot resolve length scales as short as those inside auroral arcs.

Conclusions

We conclude by summarizing the qualitative features that can be inferred from observations of FLRs undergoing PF saturation: (1) FLR saturation occurs within a few SAW periods and manifests through density depletions in the auroral zones, (2) density depletions coincide with maxima in the azimuthal magnetic field of the waves and in associated field aligned currents, (3) in the course of ponderomotive saturation, the FLR exhibits an equatorward shift (on the order of the width of the resonance) which is a direct consequence of the nonlinear phase shift between the fast mode driver and excited SAW, (4) after saturation, radial (meridional) structuring of the FLR will occur. This should lead to filamentation of the field aligned currents associated with the FLR. These features are independent of the model and can give a unified interpretation for ground and satellite measurements.

Acknowledgments. Research supported in part through the Canadian NCE Program and by the Russian Foundation of Fundamental Investigations.

References

Boehm, M. H., C. W. Carlson, J. P. McFadden, J. H. Clemmons, and F. S. Mozer, High resolution sounding rocket observations of large amplitude Alfvén waves. *J. Geophys. Res., 95,* 12,157, 1990.

Goertz, C. K., Kinetic Alfvén wave on auroral field lines, *Planet. Space Sci., 32,* 1387, 1984.

Ionson, J. A., Resonant absorption of Alfvénic surface waves and the heating of solar coronal loops, *Astrophys. J., 226,* 650, 1978.

Li, X., and M. Temerin, Ponderomotive effects on ion acceleration in the auroral zone, *Geophys. Res. Lett., 20,* 13, 1993.

Mozer, F. S., The low altitude electric field structure of discrete auroral arcs, *Geophys. Mono., 25,* 136, 1981.

Ofman, L., J. M Davila, and R. S. Steinolfson, Nonlinear studies of coronal heating by the resonant absorption of Alfvén waves, *Geophys. Res. Lett., 21,* 2259, 1994.

Samson, J. C., and R. Rankin, The coupling of solar energy to MHD cavity modes, waveguide modes, and field line resonances in the Earth's magnetosphere, *Geophys. Mono., 81,* 253, 1994.

Rankin, R., P. Frycz, V. T. Tikhonchuk, and J. Samson, Nonlinear standing shear Alfvén waves in the Earth's magnetosphere, *J. Geophys. Res., 99,* 21,291, 1994.

Rankin, R., J. C. Samson, and P. Frycz, Simulations of driven field line resonances in the Earth's magnetosphere, *J. Geophys. Res., 98,* 21,341, 1993.

Tikhonchuk, V. T., R. Rankin, P. Frycz, and J. C. Samson, Nonlinear dynamics of standing shear Alfvén waves, *Phys. Plasmas, 2,* 501, 1995.

Xu, B.-L., J. C. Samson, and W. W. Liu, Observations of optical aurora modulated by resonant Alfvén waves, *J. Geophys. Res., 98,* 11,531, 1993.

P. Frycz, R. Rankin, J.C. Samson, and V. T. Tikhonchuk, Department of Physics, University of Alberta, Edmonton, T6G 2J1, Canada

(received January 17, 1995; revised March 20, 1995; accepted April 6, 1995.)